Peer Community Journal

RESEARCH ARTICLE

Correspondence
migne@sb-roscoff.fr

Dynamics of *Fucus serratus* thallus photosynthesis and community primary production during emersion across seasons: canopy dampening and biochemical acclimation

Aline Migné[1], Gwendoline Duong[2], Dominique Menu[2], Dominique Davoult [ID],[1], and François Gévaert [ID],[2]

Abstract

The brown alga *Fucus serratus* forms dense stands on the sheltered low intertidal rocky shores of the Northeast Atlantic coast. In the southern English Channel, these stands have proved to be highly productive, particularly during emersion periods. Here, we studied the dampening effect of the canopy cover, associated with physiological and biochemical acclimation processes, that allows this species to withstand emersion stress. The *F. serratus* community primary production and the photosynthetic performance of thalli were concurrently followed in situ, throughout the midday emersion period, in different seasons and under various weather conditions. In addition, thallus samples were taken at various tidal stages to determine their content in biochemical compounds involved in photoprotective and antioxidant mechanisms. Under high light and temperature, the *F. serratus* community exhibited high aerial production rates (sometimes exceeding 1 g C m-2 h-1) that never decreased to less than 59% of the initial value during the emersion period. Under mild weather conditions, photosynthesis in thalli at the top of the canopy (measured as the relative electron transport rate) varied in response to changing incident light. Under harsh weather conditions (i.e. high light and temperature), the effective quantum yield of photosystem II (PSII) dramatically decreased in thalli at the top of the canopy, but remained high in thalli at the bottom of or within the canopy. Due to self-shading, photosynthesis was light-limited in thalli in the lowest layer of the canopy, but was effective in thalli in the intermediate layers. Photoinhibition was observed in thalli at the top of the canopy (as a dramatic decrease in the optimal photosynthetic quantum yield Fv/Fm), but not in thalli beneath the canopy. At the end of the emersion period, Fv/Fm was strongly correlated to the relative water content of thalli. The findings from our simultaneous analysis of biochemical and photosynthetic parameters suggest coordination between the xanthophyll and the ascorbate-glutathione cycles that varies with season. An accumulation of hydrogen peroxide was nevertheless observed once, indicating that oxidative stress is nonetheless possible under particularly harsh conditions.

[1]Sorbonne Université, CNRS, UMR AD2M Adaptation et Diversité en Milieu Marin, Station Biologique de Roscoff, 29680 Roscoff, France, [2]Université de Lille, CNRS, Université Littoral Côte d'Opale, UMR 8187 - LOG - Laboratoire d'Océanologie et de Géosciences, Station Marine de Wimereux, F-59000 Lille, France

CENTRE MERSENNE

Introduction

In rocky intertidal communities of temperate shores, canopy-forming macroalgae are foundation species that play a pivotal role by mitigating stressful abiotic conditions (Bulleri, 2009) and constitute highly productive systems (Mann, 1973; Niell, 1977). Sheltered shores of the Northeast Atlantic coast are characterized by stands of canopy-forming fucoids that have a distinct pattern of vertical zonation. *Fucus serratus* is usually the lowermost zone-forming fucoid (Chapman, 1995), recorded from Northern Portugal to Northern Norway (Jueterbock et al., 2013). Because the maximum shore height is reduced in southern populations, the actual thermal environment experienced by this cold-temperate species is similar at the center and southern edge of its distribution (Pearson, Lago-Leston, & Mota, 2009). Southern populations, however, are less resilient to abiotic stresses (Pearson et al., 2009) and have declined over the past decades with the increase in summer sea-surface temperatures (Casado-Amezua et al., 2019). Canopy loss induced a rapid shift to turf-forming communities, leading to the functional impoverishment of the coastal system (Alvarez-Losada, Arrontes, Martinez, Fernandez, & Viejo, 2020). Modeling the ecological niche of *F. serratus* and predicted projections of its distribution in the North Atlantic according to various climate change scenarios suggest a northward retreat of its current southern limit (Jueterbock et al., 2013). This species may thus disappear from French coasts by the end of the 21st century if it is unable to adapt to the rising temperatures (Jueterbock et al., 2014). The disappearance of this foundation species can have catastrophic consequences for its associated communities and ecosystems. For example, community metabolism was drastically reduced after the species was experimentally removed from several rocky shores of the English Channel and the North Sea (Crowe et al., 2013; Migné, Golléty, & Davoult, 2015; Valdivia, Golléty, Migné, Davoult, & Molis, 2012).

The metabolism of the *F. serratus* stand established on a rocky shore of the south of the English Channel has been investigated *in situ* at several temporal scales to model its dynamics in response to light and temperature variations (Bordeyne, Migné, Plus, & Davoult, 2020). The gross community primary production (GCP) reaches 1 g C m^{-2} h^{-1} during spring and summer midday emersions (Bordeyne, Migné, & Davoult, 2015). GCP is generally limited by light availability during immersion, and rates are systematically higher during emersion than during immersion (Bordeyne, Migné, & Davoult, 2017). Overall, despite the potentially stressful conditions inherent to exposure to air, such as high light and temperature, the production of the *F. serratus* stand remains high at the end of the emersion periods, with GCP averaging 80% of the initial level after more than 200 min of aerial exposure (Bordeyne et al., 2017). Photoinhibition has nevertheless been measured in *F. serratus* at low tide (Martinez et al., 2012). Furthermore, a severe decline in photosynthesis capacity, and an accumulation of reactive oxygen species (ROS, mainly hydrogen peroxide H$_2$O$_2$), which can cause cell damage, have been shown in low intertidal algae under simulated emersion stress (Flores-Molina et al., 2014). However, biochemical acclimation, which protects the photochemical apparatus, may allow intertidal algae to withstand emersion stress. Such acclimation includes the production and accumulation of metabolites that function as a sunscreen, protecting the thallus from harmful solar radiations, the quenching of excess excitation energy and the scavenging of ROS (Davison & Pearson, 1996). In brown algae, phenolic compounds have been suggested to act as sunscreens (e.g. Koch et al., 2016); the xanthophyll cycle (de-epoxidation of violaxanthin to zeaxanthin) is known to efficiently promote the thermal dissipation of excess excitation energy and reduce the risk of ROS generation (Harker et al., 1999); and the ascorbate-glutathione cycle may be the main pathway for scavenging H$_2$O$_2$ (Nan, Zhang, Sheng, & Zhang, 2016). In canopy-forming macroalgae, the stress of aerial exposure may also be limited through self-covering (Monteiro et al., 2017), preventing algae from overheating, desiccation and photoinhibition (Fernandez et al., 2015).

The multidimensional structure of macroalgae stands has been demonstrated to allow sub-optimal distribution of underwater light among thalli (Binzer & Sand-Jensen, 2002), and the temporal and spatial supplementation between thalli for light absorbance has been shown to enhance photosynthetic production of shallow water communities (Sand-Jensen, Binzer, & Middelboe, 2007) or intertidal communities under immersion (Tait & Schiel, 2011). Canopy protection and complementarity between thalli from different layers of the *F. serratus* stand have also been proposed to explain how primary production can be favored during aerial exposure under high light (Bordeyne et al., 2017), but this remains to be demonstrated. During emersion periods, the horizontal layering of thalli implies a steep attenuation

of light within the canopy. Likewise, *F. serratus* thalli exhibited effective light harvesting at low irradiance in laboratory experiments (e.g. Lichtenberg & Kuhl, 2015). However, to understand how self-covering can enhance the primary production of the whole community, the dynamics of photosynthetic capacity has to be investigated in a naturally structured stand, in combination with an integrated measurement of the metabolism of the whole community (Tait, Hawes, & Schiel, 2017).

In the present survey, the aerial production of the community was assessed *in situ* by measuring carbon fluxes inside closed chambers. We assessed the photosynthetic activity of thalli from different layers of the canopy concurrently by measuring chlorophyll *a* fluorescence. In addition, we evaluated the involvement of biochemical compounds in photoprotective mechanisms, the induction of ROS and the activation of the antioxidant system by quantifying the phenolic compounds, xanthophyll cycle pigments (violaxanthin, antheraxanthin and zeaxanthin), H_2O_2 and ascorbate and glutathione present in thalli. The study aimed to 1) describe the *in situ* dynamics of the *F. serratus* community primary production and the photosynthetic performance of thalli throughout the midday emersion period under various environmental conditions (according to the season and the weather); 2) investigate the biochemical acclimation patterns of *F. serratus* across seasons and during emersion. We tested the hypothesis that, depending on the prevailing environmental conditions, thalli at the top of the canopy develop photoprotective and/or scavenging mechanisms.

Methods

Study site, environmental conditions and experiments schedule

This study was performed on the shore located in front of the Roscoff Marine Station (48°43.743'N, 3°59.407'W) in the southwestern part of the English Channel. This location experiences seasonal variations in environmental parameters typical of the temperate part of the Northern Hemisphere (Bordeyne et al., 2015). Photosynthetically available radiation (400-700 nm, PAR) and air temperature are recorded continuously by a weather station (flat quantum sensor SKP215, Skye Instruments LTD) located on the building of the Roscoff Marine Station and averaged over 15 min. Seawater temperature and nutrient concentrations are measured fortnightly at the Roscoff-Estacade sampling point of the SOMLIT network (data available online at https://somlit.fr/visualisation-des-donnees/).

At the low mid-intertidal level of the shore, the semi-sheltered boulder reef is typically characterized by a dense stand of the fucoid *Fucus serratus* (about 70 ind m^{-2} accounting for 2 to 13 kg$_{FW}$ m^{-2} according to the season, Bordeyne, 2016). During emersion periods, the long *F. serratus* thalli (averaging 38 cm, Munda & Kremer, 1997) form a layered canopy which height can reach several decimetres. During spring tides, the middle part of this stand (about 3 m above chart datum) is exposed to air for about 4 h around noon. Two types of experiment were carried out during the emersion period of spring tides, occurring around midday under various environmental conditions (Table 1). In the first type of experiment, photosynthesis was compared between thalli at the top of the canopy and thalli at the bottom of the canopy: two experiments were performed under high and relatively constant light (Exp A the 26th May and Exp B the 22nd August 2017), two under high but more variable light (Exp C the 27th May and Exp D the 23rd August 2017) and one under low light (Exp E the 04th December 2017). In the second type of experiment, photosynthesis was compared between thalli at the top of the canopy and thalli in intermediate layers: one experiment was performed under high and relatively constant light (Exp F the 13th August 2018) and one under low light (Exp G the 05th December 2017).

During the emersion period of each date of experiments, PAR was measured at the level of the substratum using a flat quantum sensor (LiCor SA-190) and recorded every minute. PAR reaching thalli at the bottom of or within the *F. serratus* canopy was measured at the same time as fluorescence using a mini flat quantum sensor (Walz). The air temperature was measured at the *Fucus* stand and recorded every minute using two HOBO loggers placed respectively above (T_{ab}) and below (T_{be}) the canopy. A canopy temperature buffering index (TBI) was then calculated every minute as TBI = ($T_{ab} - T_{be}$) / T_{ab}.

Table 1. Environmental conditions for the two types of experiments, comparison between thalli at the top and the bottom of the canopy (I) and at the top and in intermediate layer of the canopy (II). Low tide time (universal time) and height (above chart datum) and total emersion period at the 3 m shore level predicted in Roscoff on each experiment date (YY/MM/DD). Light and temperature recorded at different layers in the *Fucus serratus* canopy during the measurement period.
PAR: photosynthetically available radiations, rETR: relative electron transport rate, TBI: canopy temperature buffering index

Type of experiment	I. Bottom vs. Top					II. Intermediate layer vs. Top	
Code name	Exp A	Exp B	Exp C	Exp D	Exp E	Exp F	Exp G
Date	17/05/26	17/08/22	17/05/27	17/08/23	17/12/04	18/08/13	17/12/05
Low tide time	11:36	11:43	12:23	12:25	11:35	12:45	12:23
Low tide height (m)	0.85	1.15	0.85	1.10	0.90	0.80	0.80
Emersion period	9:35-13:27	9:48-13:27	10:23-14:15	10:30-14:11	9:36-13:26	10:45-14:36	10:22-14:16
Measurement period	10:15-12:55	10:40-13:00	11:00-13:50	11:00-13:40	10:00-13:10	11:30-14:15	10:35-14:00
Light (PAR, µmol m^{-2} s^{-1})							
Mean incident PAR	1859	1613	1287	1276	305	1628	200
Mean PAR for rETR							
Top canopy layer	1854	1588	1312	1225	293	1588	196
Intermediate layer						146	38
Bottom canopy layer	11	12	13	10	6		
Temperature (T, °C)							
Mean T above canopy	31.6	32.9	25.9	28.3	14.0	29.9	12.3
Mean T below canopy	20.6	23.3	18.7	22.2	12.0	20.9	11.6
Mean TBI	0.35	0.29	0.28	0.22	0.14	0.30	0.06

Community primary production

Productivity was assessed at the *F. serratus* community scale by measuring carbon dioxide (CO_2) fluxes inside benthic chambers. At the beginning of emersion period, three chambers were haphazardly positioned (approximately 2 m apart) to account for spatial variability. Each chamber (made of a transparent Perspex® dome with a 0.3 x 0.3 m transparent air-tight Perspex® base, total volume 17.7 L) was sealed to the substratum (using sand) and was connected to an infrared CO_2 gas analyzer (LiCor Li-820) in a closed air circuit (with a flow of about 1 L min^{-1}). CO_2 air concentration (μmol_{CO2} mol$_{air}^{-1}$) was recorded every 15 s for 5 to 10 min during incubation to calculate CO_2 fluxes as described in Migné *et al.* (2002). Measurements were performed at ambient light and in darkness by covering the chambers to estimate net community production (NCP) and community respiration (CR), respectively. Benthic chambers were opened between two consecutive incubations to renew the ambient air. Gross community production (GCP), calculated as the sum of NCP and CR, was expressed in carbon units (mg C m^{-2} h^{-1}) assuming a molar volume of 22.4 L mol^{-1} at standard temperature and pressure and a molar mass of 12 g C mol$_{CO2}^{-1}$. Successive sets of light and dark incubations were carried out from the onset of emersion period to the return of seawater at intervals of ca. 30 min.

Thalli photosynthesis

Photosynthesis of *F. serratus* thalli was assessed *in situ* using a pulse-amplitude modulated (PAM) fluorometer (Diving PAM, Walz). The fluorescence signal was always taken from the same place in the middle of the thallus for three individuals, haphazardly selected among thalli from the top of the canopy and three other individuals from the bottom of the canopy or from an intermediate layer of the canopy. Thalli were selected according to the incident irradiance reaching them: approximately 1% and 20% of incident PAR at the bottom and within the intermediate layer of the canopy respectively. The effective quantum yield of photosystem II (Φ_{PSII}) was measured under ambient light. The optical fibers were mounted in a home-made holder that kept the distance between the fiber optics and the algal tissue constant and standard, with a 60° angle, avoiding shading or darkening (Figure 1). Φ_{PSII} was calculated as ($F_m'-F_t$)/F_m' (Genty, Briantais, & Baker, 1989), where F_m' is the maximal level of fluorescence measured during a single saturating pulse of white light (0.8 s), and F_t is the steady-state level of fluorescence measured immediately before the flash, under actinic illumination. Φ_{PSII} estimates the relative electron transport rate (rETR in µmol electrons m^{-2} s^{-1}, hereafter referred to as µmol e$^-$ m^{-2} s^{-1}) as $\Phi_{PSII} \times$ PAR $\times$ 0.5, where PAR is the photosynthetically available radiation (in µmol photons m^{-2} s^{-1}), and 0.5 is a correction

factor based on the assumption that the incident photons are absorbed equally by the pigments of the two photosystems. rETR was measured from the onset of emersion period to the return of seawater at intervals of ca. 30 min. The optimal quantum yield of PSII photochemistry was measured on dark-adapted thalli and was calculated as $F_v/F_m = (F_m – F_0)/F_m$ (Genty et al., 1989), where F_v is the variable fluorescence, F_0 is the minimal level of fluorescence, and F_m is the maximal fluorescence obtained during the application of a saturating pulse of white light (0.8 s). Thalli were dark-adapted by applying a leaf clip on the samples for 10 min, a period estimated to be long enough to allow the complete re-oxidation of the primary quinone electron acceptor of PSII (Kalaji *et al.*, 2014). F_v/F_m assesses the extent of photoinhibition (Maxwell & Johnson, 2000) and was measured at the beginning, middle and end of the emersion period.

Relative water content of thalli

Six haphazardly selected *F. serratus* thalli were detached from the rock at the onset of emersion to monitor their relative water content (RWC) during the emersion period. Three were placed at the bottom of or inside the canopy, and three were placed at the top of the canopy. The weight (W) of each thallus was measured in the field at the beginning, middle and end of the emersion period. Brought back to the laboratory, the thalli were rehydrated overnight to assess their fresh weight (FW) and then dried for 48 h at 60°C to assess their dry weight (DW). The relative water content of a thallus was calculated as the part of total water content [(W-DW)/(FW-DW)] at the beginning, middle and end of emersion.

Figure 1. *In situ* survey of fluorescence of thalli beneath the canopy

Biochemical parameters

Thallus samples were taken at the beginning, middle and end of the emersion period, from three individuals haphazardly selected at the top and three thalli haphazardly selected from the bottom (or in an intermediate layer) of the canopy, and immediately placed in the dark and frozen in liquid nitrogen until further biochemical analysis.

For the analysis of chlorophyll and xanthophyll cycle pigments, thallus samples (disks of 8 mm diameter) were first gently patted dry to remove epiphytes. Pigments were extracted by grinding the disks in a cold mortar with methanol and small drops of methylene chloride under dim light. Extracts were centrifuged (5 min, 13 000 rpm) and supernatants were collected and filtered on polytetrafluoroethylene membranes

(0.2 μm) and dry-evaporated under nitrogen. Salt contents of the extract were removed from the pigment solution in a methylene chloride:distilled water mixture (50:50, v/v) (salts stay in the aqueous phase, and pigments are found in the organic phase). The organic phase was then evaporated with nitrogen and dissolved again in 40 μL methanol just before injection. Pigment analysis was performed using high performance liquid chromatography (HPLC) (Shimadzu, Nexera XR) with a reverse-phase column (C18 Allure, Restek). Briefly, 20 μL were injected, and separation was carried out with a solvent delivery profile adapted from Arsalane *et al*. (1994). The conversion of violaxanthin (V), a pigment with no photoprotective properties into antheraxanthin (A) and zeaxanthin (Z), which are involved in the dissipation of energy into heat (Bilger & Bjorkman, 1990), was estimated by calculating the de-epoxidation ratio: $DR = (A + Z)/(V + A + Z)$.

For the analysis of the other compounds, thallus samples (pieces of about 10 g_{FW}) were patted dry, lyophilized and grounded. Phenolic compounds were determined using a protocol adapted from Ratkevicius *et al*. (2003) and from Contreras *et al*. (2005): 0.05 g of ground lyophilized thallus samples were homogenized with a glass pestle in an Eppendorf tube containing 1 mL phosphate buffer 0.1 M pH = 7. Homogenates were centrifuged (10 min, 13 000 rpm) and aliquots of 100 μL of the supernatants were added to a reaction mixture containing 3% of sodium carbonate and 0.3 M Folin–Ciocalteau reagent in a final volume of 1 mL. After an incubation period of 2 h at room temperature, the absorbance was measured at 765 nm (UV-2450, UV-VIS, Shimadzu). Total phenolic compounds (PC) were expressed in g of nano-equivalents of gallic acid per 100 g of DW (% DW) using a calibration curve prepared with gallic acid. Hydrogen peroxide (H_2O_2) concentrations were determined using a protocol adapted from Lee and Shin (2003): 0.05 g of ground lyophilized thallus samples was homogenized with a glass pestle in an Eppendorf tube containing 1 mL of trichloroacetic acid (TCA). Homogenates were centrifuged (10 min, 13 000 rpm) and aliquots of 0.2 mL of supernatant were added to a reaction mixture containing 0.2 mL of phosphate buffer and 0.8 mL of potassium iodide. After an incubation period of 1 h in darkness, absorbance was measured at 390 nm (UV-2450, UV-VIS, Shimadzu). The equivalent concentration was obtained by using a standard curve prepared with TCA and a solution of 0.01 M H_2O_2. Ascorbate (Asc) concentrations were determined using a protocol adapted from Hodges *et al.* (1996): 0.05 g of ground lyophilized thallus samples was homogenized with a glass pestle in an Eppendorf tube containing 1 mL of 2.5 M perchloric acid. Homogenates were centrifuged (10 min, 13 000 rpm) and aliquots of 0.1 mL of supernatant were added to 5 μL of 100 mM dithiothreitol. After an incubation period of 1 h at room temperature, the reaction was stopped by adding 5 μL of 5% *n*-ethylmaleimide and 900 μL of a reaction mixture containing 2% TCA, 8.8% orthophosphoric acid, 0.2% 2-2'-bipyridyl and 10 mM iron chloride and then incubated for 1 h at 40°C. Absorbance was measured at 525 nm (UV-2450, UV-VIS, Shimadzu). The equivalent concentration was obtained by using standard curves prepared with derivative L-AA standard. Glutathione (Glu) concentrations were determined using a protocol adapted from Hodges *et al.* (1996): 0.05 g of ground lyophilized thallus samples was homogenized with a glass pestle in an Eppendorf tube containing 1 mL of 5% 5-sulfosalicylic acid dehydrate. Homogenates were centrifuged (10 min, 13 000 rpm) and aliquots of 0.1 mL of supernatant were added to 150 μL of 500 mM phosphate buffer (pH 7.5). The neutralized extract was added to a reaction mixture containing 100 mM phosphate buffer (pH 7.0), 0.15 mM NADPH, 60 μM DNTB and 0.66 U glutathione reductase for the quantitative analysis of total Glu and then incubated for 1 h at 37°C. Absorbance was measured at 412 nm (UV-2450, UV-VIS, Shimadzu). The equivalent concentration was obtained by using standard curves prepared with an L-Glutathione reduced BioXtra (GSH) standard.

Data analysis

Pearson correlation was tested between the canopy temperature buffering index (TBI) and the mean temperature above canopy (T_{ab}). A principal component analysis (PCA) was performed on the mean values of biochemical parameters (DR, H_2O_2, Asc, Glu), relative water content (RWC), and optimal quantum yield (F_v/F_m) measured at the end of the emersion period on the different experiment dates to explore a seasonal pattern. The seasonal acclimation of *F. serratus* was also investigated based on phenolic contents (PC) and xanthophyll cycle pigments (V + A + Z), normalized to the chlorophyll *a* content, for each of the four months of measurement (May, August and December 2017 and August 2018). Data obtained from thalli sampled at the beginning of emersion on two consecutive days were pooled. Kruskal-Wallis tests (non-parametric

equivalent to ANOVA) and post-hoc pairwise Wilcoxon tests (with the Holm method for p-value adjustment) were used to analyze differences between the four months of measurement.

Results

Environmental conditions

Across the whole experiment (May 2017-August 2018), air temperature recorded by the weather station ranged from -3.2 to 26.2 °C. Monthly mean air temperature varied seasonally (16.5 °C in August 2017, 6.3 °C in February 2018 and 17.5 °C in July 2018). Samples from the Roscoff-Estacade point of the SOMLIT network showed typical seasonal variation in monthly mean seawater temperature (16.4 °C in August 2017, 9.3 °C in February 2018 and 16.3 °C in August 2018) and in monthly mean inorganic nitrogen concentration (0.29 ± 0.01 µmol L^{-1} in May 2017, 9.40 ± 2.06 µmol L^{-1} in January 2018 and 0.74 ± 0.59 µmol L^{-1} in July 2018).

During the experiments, mean air temperature measured just above the *F. serratus* canopy (T_{ab}) varied from 12.3 to 32.9 °C and the mean canopy temperature buffering index (TBI) varied from 0.06 to 0.35 (Table 1). TBI was positively correlated with T_{ab} ($r = 0.928$, $n = 7$, $p < 0.01$). Incident PAR measured at the level of the substratum varied according to the season and weather conditions (Figures 2 & 3), with a mean in the range of 200-1859 µmol m^{-2} s^{-1} (Table 1).

Community primary production

Mean gross community primary production (GCP) higher than 1 g C m^{-2} h^{-1} was measured at the beginning of emersion on three dates (Figures 2 & 3): 1.28 g C m^{-2} h^{-1} on 26 May 2017 (Exp A), 1.26 g C m^{-2} h^{-1} on 22 August 2017 (Exp B) and 1.03 g C m^{-2} h^{-1} on 13 August 2018 (Exp F). On these dates, which are the ones with the highest temperature and incident light (Table 1), GCP decreased during the emersion period, representing respectively 66, 74 and 59% of the initial value at the end of the emersion period. On 27 May (Exp C), 23 August (Exp D) and 05 December 2017 (Exp G), GCP remained relatively stable during the emersion period (averaging 0.91, 0.80 and 0.43 g C m^{-2} h^{-1}, respectively). On 04 December 2017 (Exp E), GCP varied according to the incident light (reaching 0.92 g C m^{-2} h^{-1} when PAR peaked at 800 µmol m^{-2} s^{-1}).

Thalli photosynthesis

The highest relative electron transport rate (rETR) averaged 247 µmol e^- m^{-2} s^{-1} and was measured in thalli at the top of the canopy at the beginning of emersion on 26 May 2017 (Exp A, Figure 2). In thalli at the top of the canopy, rETR dramatically decreased during emersion in May and August (Exp A, B, C, D, Figure 2 & Exp F, Figure 3). Mean rETR decreased to values lower than 20 µmol e^- m^{-2} s^{-1} due to very low values of effective quantum yield: Φ_{PSII} was less than 0.05 (and even less than 0.01 on 13 August 2018, Exp F). In December, Φ_{PSII} remained higher than 0.60, and rETR varied with the incident light on 04 December (reaching 145 µmol e^- m^{-2} s^{-1} when PAR peaked at 800 µmol m^{-2} s^{-1}, Exp E, Figure 1) and remained relatively stable on 05 December (averaging 65 µmol e^- m^{-2} s^{-1}, Exp G, Figure 2). In thalli at the bottom of the canopy, Φ_{PSII} averaged 0.75 across all measurement dates, but rETR remained virtually nil (Figure 3) due to the very low PAR (Table 1). In thalli in the intermediate layers of the canopy, Φ_{PSII} averaged 0.72 in August and 0.75 in December, and rETR averaged 53 and 14 µmol e^- m^{-2} s^{-1} in August (Exp F) and December (Exp G), respectively (Figure 3). In August 2018, rETR in the intermediate layers of the canopy was higher than at the top of the canopy for most of the emersion period.
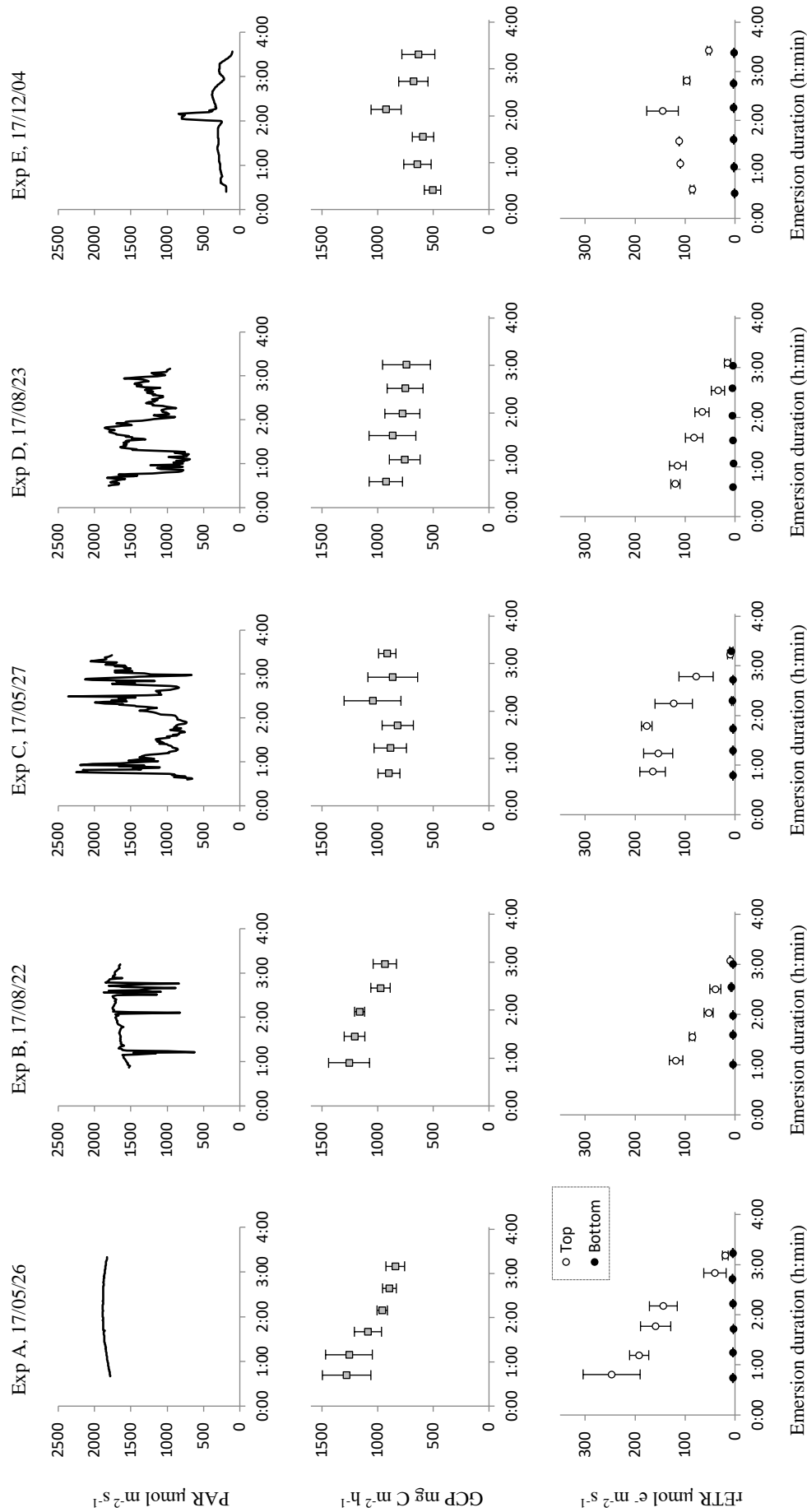
Figure 2. Incident light (as photosynthetically available radiation, PAR), gross community primary production (GCP, mean ± se, n = 3), and relative electron transport rate (rETR, mean ± se, n = 3) of thalli at the top and bottom of the *Fucus serratus* canopy measured during emersion on different dates
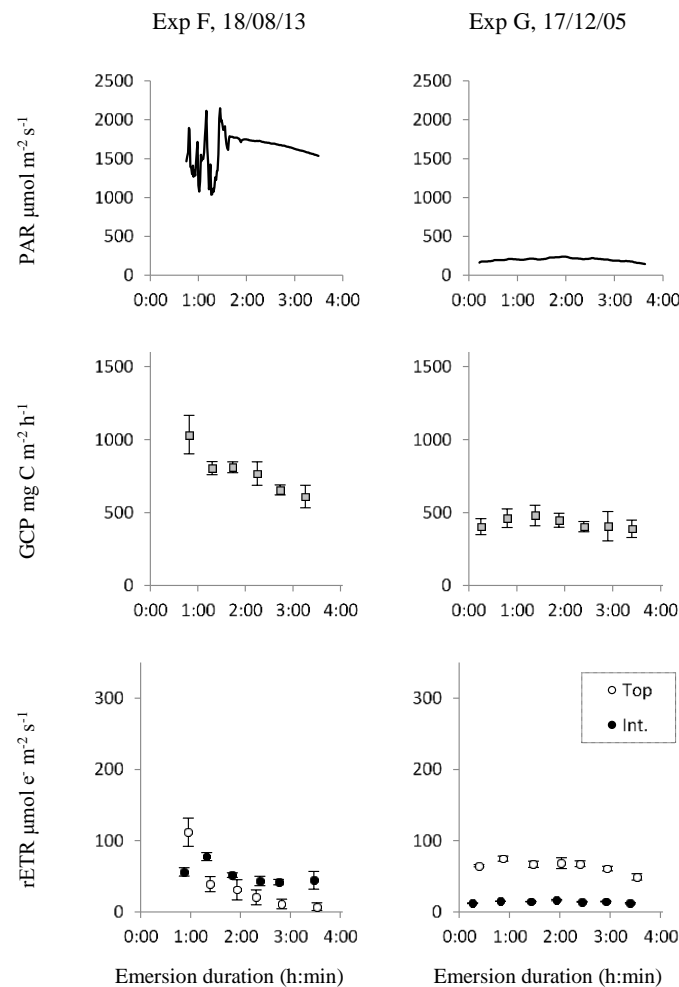
Figure 3. Incident light (as photosynthetically available radiation, PAR), gross community primary production (GCP, mean ± se, n = 3), and relative electron transport rate (rETR, mean ± se, n = 3) of thalli at the top and intermediate layers of the *Fucus serratus* canopy measured over emersion on different dates

The optimal quantum yield (F_v/F_m) measured in thalli at the top of the canopy decreased during emersion period in May and August (Exp A, B, C, D, Figure 4 & Exp F, Figure 5), even reaching a null value in August 2018 (Exp F), and remained stable (higher than 0.73) in December (Exp E, Figure 4 & Exp G, Figure 5). In thalli at the bottom of the canopy (Figure 4) and in the intermediate layers of the canopy (Figure 5), mean F_v/F_m always remained higher than 0.65.
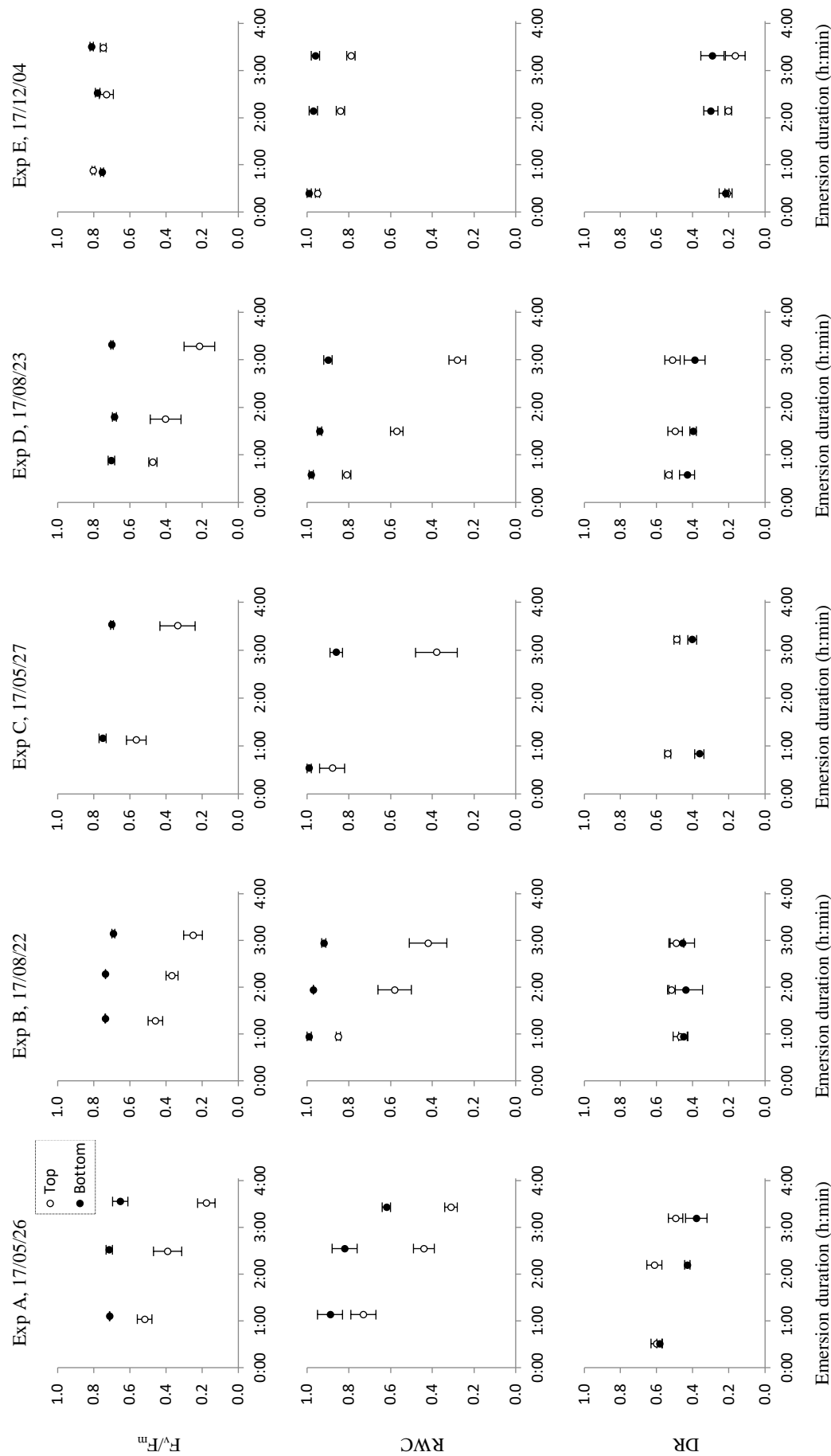
Figure 4. Mean (± se, n = 3) optimal quantum yield of PSII (F_v/F_m), relative water content (RWC), and de-epoxidation ratio (DR) measured during emersion on thalli at the top and bottom of the *Fucus serratus* canopy on different dates
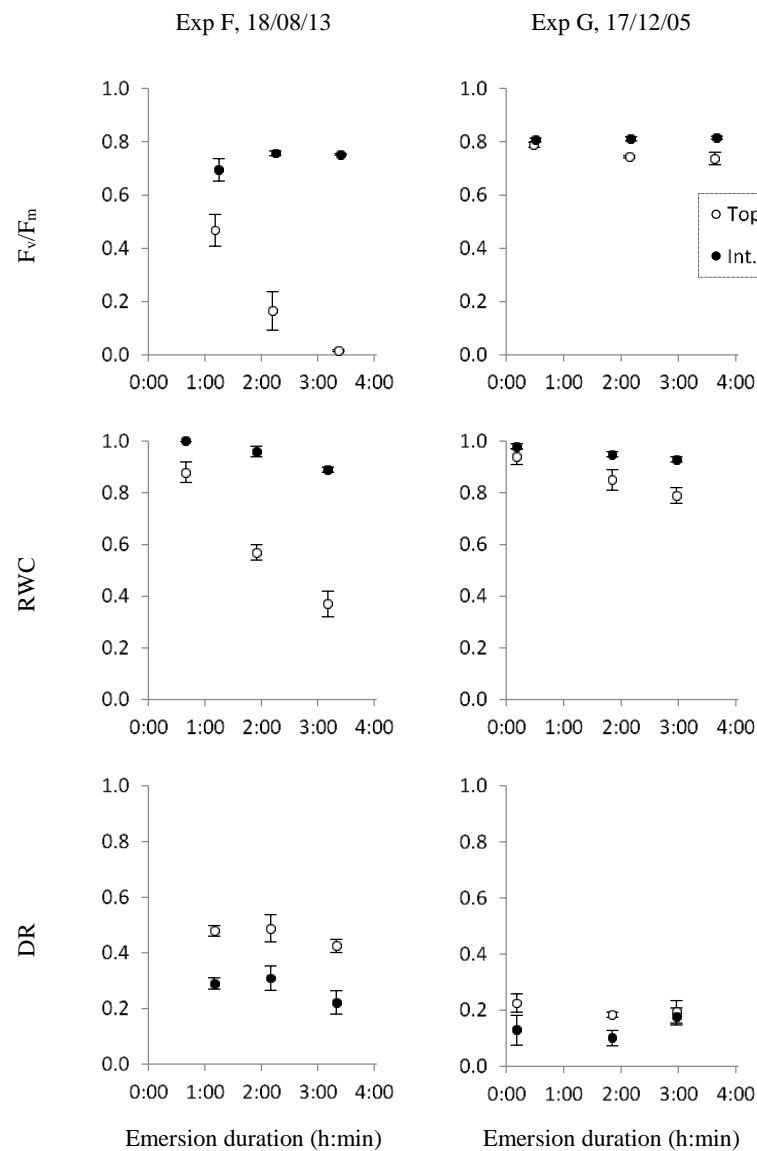
Exp F, 18/08/13   Exp G, 17/12/05

Figure 5. Mean (± se, n = 3) optimal quantum yield of PSII (Fv/Fm), relative water content (RWC) and de-epoxidation ratio (DR) measured during emersion on thalli at the top and intermediate layers of the *Fucus serratus* canopy on different dates

Relative water content of thalli

The relative water content (RWC) measured in thalli at the top of the canopy decreased during emersion periods. After about 3 h of emersion, RWC reached values in the range [0.28-0.42] in May and August (Exp A, B, C, D, Figure 4 & Exp F, Figure 5), and 0.79 in December (Exp E, Figure 4 & Exp G, Figure 5). In thalli at the bottom and intermediate layers of the canopy, mean RWC generally slightly declined during emersion. After about 3 h of emersion, it reached values ranging from 0.86 to 0.96, except on 26 May 2017 (Exp A) when it reached 0.62.

Biochemical parameters

The de-epoxidation ratio (DR) tended to decrease during the emersion period on 26 May 2017, notably at the bottom of the canopy (Exp A, Figure 4). No trends were observed for DR on the other days (Exp B, C, D, E, Figure 4; Exp F, G, Figure 5). Globally, mean DR was relatively high in May and August (0.45 ± 0.02) and low in December (0.20 ± 0.02).

The hydrogen peroxide (H_2O_2), ascorbate (Asc) and glutathione (Glu) contents of thalli at the top of the canopy generally did not increase during the emersion period (Appendix 1), except on 26 May 2017 (Exp A, Glu increased from 0.87 ± 0.12 to 1.38 ± 0.13 µmol g_{DW}^{-1}), on 22 August 2017 (Exp B, Asc increased from 6.49 ± 0.29 to 9.17 ± 1.69 µmol g_{DW}^{-1}) and on 13 August 2018 (Exp F, H_2O_2 increased from 3.85 ± 0.41 to 5.02 ± 0.64 µmol g_{DW}^{-1}). Some notable increases were also observed in thalli at the bottom of the canopy in May and August.

The principal component analysis (PCA), performed on the mean values of biochemical parameters (as well as of RWC and F_v/F_m) measured at the end of the emersion period highlighted the strong correlation between F_v/F_m and RWC (r = 0.938, n = 14, p < 0.001, Figure 6a). A seasonal pattern appeared in thalli at the top of the canopy (Figure 6b), with high DR characterizing summer samples (Exp B, D, F) and high Asc and Glu characterizing spring samples (Exp A, C).

The phenolic content (PC) of *F. serratus* thalli varied significantly according to the month of measurement (Kruskal Wallis test, p < 0.001), with a significantly higher mean value in December 2017 (3.31% DW, post-hoc test, p < 0.01) than in any other month of measurement (Figure 7a).

The pool of pigments involved in the xanthophyll cycle normalized to the chlorophyll *a* content (VAZ/Chl*a*) varied significantly with month of measurement (Kruskal Wallis test, p < 0.001), the highest value was observed in May 2017 (0.23), and the lowest in December 2017 (0.15, Figure 7b).

Discussion

Community primary production and photosynthesis

The studied intertidal *Fucus serratus* stand exhibited high aerial production rates (sometimes exceeding 1 g C m^{-2} h^{-1}) under high light and temperature (Figures 2 & 3). During the emersion period, production rates never decreased to less than 59% of the initial value. This pattern was already highlighted in a previous study (Bordeyne et al., 2017), but our study demonstrates that production is maintained at a relatively high rate due to the dampening effect of the canopy on temperature and light and to various acclimation mechanisms. Canopy shading helps prevent the thallus from overheating and retains humidity during emersion, and self-covering in intertidal stand of macroalgae has been considered as an intraspecific facilitation mechanism that protects the algae from photoinhibition (Fernandez et al., 2015). The temperature buffering index (TBI) measured here was positively correlated with air temperature. Under the harshest conditions of the present survey, TBI was comparable to that measured on more southern *Fucus* species stands, situated at higher shore levels (Monteiro et al., 2017). We did not measure the humidity buffering index here, but regardless of the encountered weather conditions, the relative water content (RWC) was higher in thalli placed below the canopy than in thalli at the top of the canopy, confirming the canopy dampening effect. The previously proposed hypothesis of intraspecific facilitation as a mechanism regulating the production of intertidal macroalgae stands (Bordeyne *et al.*, 2017) is validated by the physiological measurements presented here. During emersion under mild conditions, photosynthesis, measured as the electron transport rate (rETR), varied in thalli at the top of the canopy in response to changing incident light (Exp E, Figure 2). This variation confirms the capacity of the species for short-term photoacclimation, as already shown in laboratory experiments (Lichtenberg & Kuhl, 2015). In contrast, during emersion under harsh conditions, the efficiency of photosystem II photochemistry dramatically decreased in thalli at the top of the canopy. Under these conditions, the efficiency of the photosystem II photochemistry nonetheless remained high in thalli at the bottom of or within the canopy. Photosynthesis was limited in the lowest layer of thalli due to self-shading which prevented light from reaching them (only approximately 1% of the incident irradiance reached the bottom of the canopy), but was effective in the intermediate layers under relatively low local irradiance (approximately 20% of incident irradiance). In the Roscoff *F. serratus* stand, thalli are typically long, wide, ramified and deeply serrated (Munda & Kremer, 1997). This morphology helped distribute the available irradiance within the canopy and also protected the photosynthetic tissues within the canopy from emersion stress. The unpredictable

nature of the distribution of light within the canopy nevertheless involved acclimation of the photosynthetic apparatus.
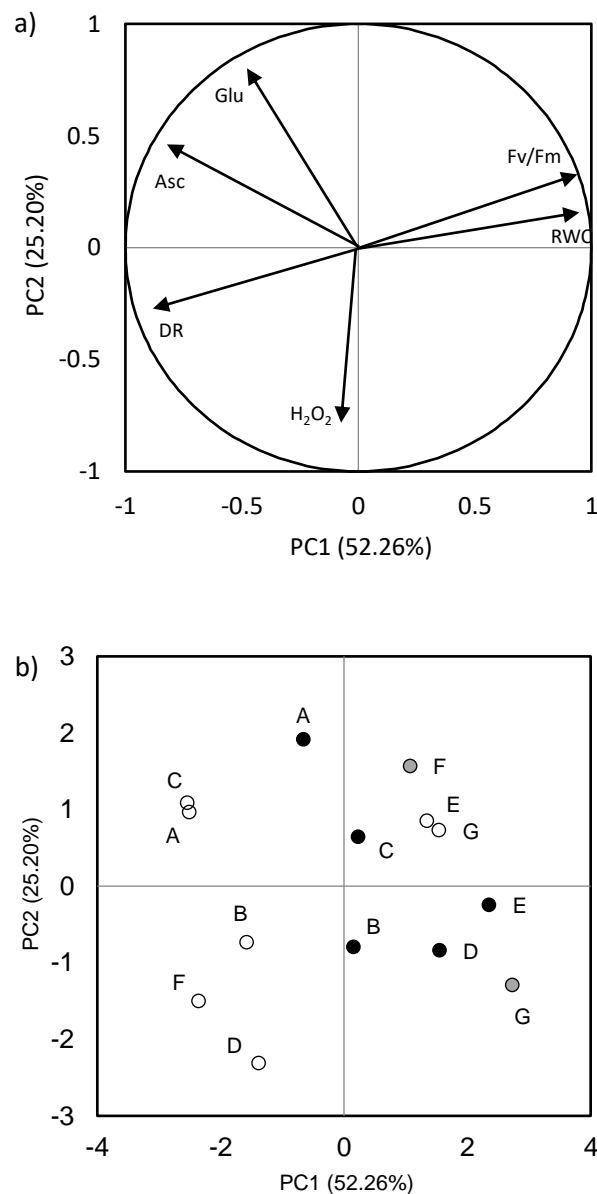

Figure 6. Projection onto the PC1-PC2 plane (a. Variables map, b. Objects map) of the results of principal component analysis (PCA) performed on the mean values of biochemical parameters (de-epoxidation ratio (DR), hydrogen peroxide (H_2O_2), ascorbate (Asc), and glutathione (Glu) contents), relative water content (RWC), and optimal quantum yield (F_v/F_m) measured at the end of the emersion period on May (A, C), August (B, D, F) and December (E,G) in thalli from different layers of the *Fucus serratus* canopy: top (white), bottom (dark) and intermediate (grey)
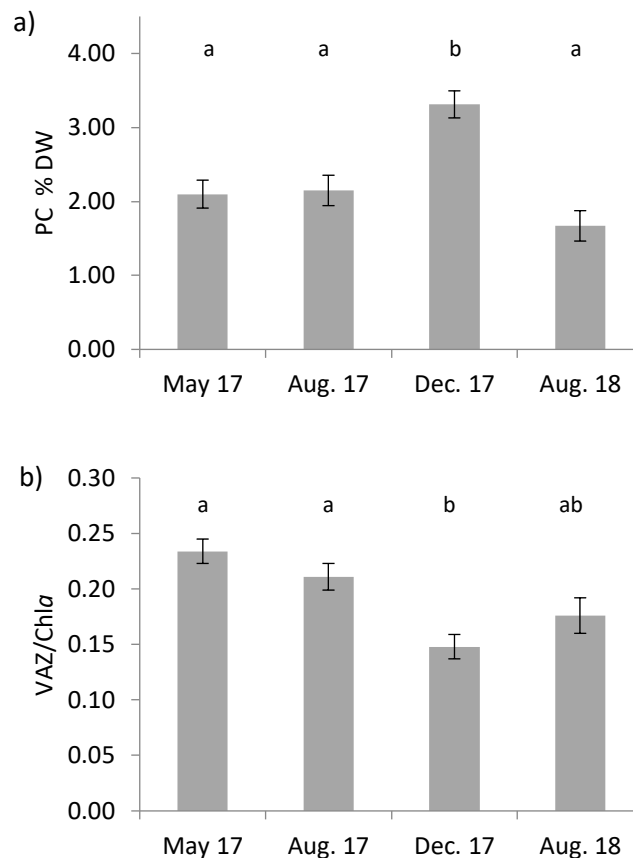
Figure 7. Mean (± se, n = 12 in May, August and December 2017 and n = 6 in August 2018) contents of phenolic compounds (a) and pigments involved in the xanthophyll cycle normalized to the chlorophyll *a* content (b) in each of the four months of measurement. Different letters represent significant differences between months of measurements (post-hoc test, p < 0.01).

The optimal photosynthetic quantum yield (F_v/F_m) also dramatically decreased during emersion periods of spring and summer in thalli at the top of the canopy, but not in thalli beneath the canopy (at the bottom, Figure 4, or in intermediate layers, Figure 5). However, photoinactivation kinetics varied with the prevailing weather conditions. The strong correlation between F_v/F_m and RWC measured in thalli at the end of the emersion period (Figure 6a) suggests that photoinactivation of PSII is mainly governed by thallus dehydration. Photoinactivation of PSII by desiccation has been proposed as a mechanism to prevent an overload of the photosynthetic apparatus in intertidal algae under high light during emersion at low tide, therefore, protecting them from photodamage (Huppertz, Hanelt, & Nultsch, 1990). Laboratory experiments performed under high light and high temperature (Fernandez et al., 2015; Martinez et al., 2012) suggest that the recovery of the photosynthetic capacity of *F. serratus* thalli exposed during emersion may be not complete before the onset of the next midday low tide. The same thalli are, however, unlikely to be at the top of the canopy in consecutive low tides and inhibition can be reversed by self-shading. F_v/F_m at the top of the canopy reached a null value at the end of the emersion period on 13 August 2018 (Exp F, Figure 5). Contrarily to August 2017 (Exp B), harsh conditions, notably high air temperatures, occurred not only the day of measurement on 13 August 2018 (Exp F), but also the previous days, and we hypothesize a possible cumulative effect due to overheating during this spring-tide period. Canopy protection may therefore not be sufficient to allow this intertidal alga to withstand several consecutive harsh midday conditions during a spring-tide cycle.

Biochemical acclimation

Significant changes in phenolic content and pigment content between the different periods of measurements (Figure 7) indicate a seasonal biochemical acclimation of *F. serratus*. Canopy-forming algae,

in particular fucoids, are known to be rich in phenolic compounds, which have been suggested to act as a sunscreen against harmful solar radiations (high PAR and UV). Therefore, we expected to observe a seasonal pattern in phenolic compounds in *F. serratus* thalli, with maximum values in summer as previously observed in the same geographical area (Connan, Goulard, Stiger, Deslandes, & Gall, 2004). However, phenolic compounds have various functions (including protection against grazers and epiphytes) which may lead to different seasonal trends. Furthermore, environmental factors may affect their concentration in brown algae (Ragan & Jensen, 1978; van Hees, Olsen, Wernberg, Van Alstyne, & Kendrick, 2017). For example, both field surveys and experimental studies on intertidal seaweeds suggest that the synthesis of phenolic compounds depends on nitrogen availability (Yates & Peckol, 1993) or is inhibited by high temperatures (Mancuso et al., 2019; Mannino, Vaglica, Cammarata, & Oddo, 2016). Here, as in a Norwegian *Fucus vesiculosus* population (Ragan & Jensen, 1978), high contents were measured under low temperature and high nitrogen availability (in December), and low contents were measured under high temperature and low nitrogen availability (in May and August), which does not support the idea of a photoprotective role for phenolic compound accumulation. Because the xanthophyll cycle is the principal non-photochemical quenching mechanism in brown algae (Harker *et al.*, 1999), we expected to observe an accumulation of xanthophyll pigments in spring and summer. The xanthophyll pigment content normalized to the chlorophyll *a* content measured in December (0.15) appeared nevertheless relatively low compared with the values (0.23-0.26) reported for a population sampled in winter in southwest England (Nielsen & Nielsen, 2010). In that more northern population, the phenolic content was, in contrast, particularly low (between 0.50 and 1.40% DW). The opposite trends in the xanthophyll pigments content and phenolic content observed here between seasons, as well as between the two populations in winter, indicate that there may be complementary photoprotection mechanisms and different strategies in different *F. serratus* populations. In intertidal fucoids, the photoprotective role of phenolic compounds may depend not only on their sunscreen effect, but also on their antioxidant capacities (Connan, Deslandes, & Gall, 2007), and zeaxanthin may also have antioxidative properties (Nielsen & Nielsen, 2010).

Violaxanthin de-epoxidation is a rapid protection mechanism of the photosynthetic apparatus by excess light energy dissipation (Hanelt, 1996), and we expected this mechanism to be activated in thalli exposed to high light at the onset of emersion. Relatively high de-epoxidation ratio (DR) values were however measured not only in thalli at the top of the canopy, but also in thalli beneath the canopy at the beginning of the emersion period in spring and summer (Figures 4 & 5). These high values suggest that the mechanism is activated as a response to supersaturating light irradiance in very low water depth at the end of immersion. The high correlation between the DR values at the beginning of emersion and the prevailing PAR just before emersion (Pearson correlation r = 0.950, n = 7, p < 0.001, Appendix 2) tends to confirm this hypothesis. Although high temperature and dehydration may have made additive contributions to stress, DR did not increase with decreasing F_v/F_m in thalli lying at the top of the canopy during emersion. In contrast, desiccation and high temperature may have lowered DR values, as shown in the uppermost midlittoral species *Pelvetia canaliculata* (Fernandez-Marin, Miguez, Maria Becerril, & Ignacio Garcia-Plazaola, 2011; Harker et al., 1999). The ascorbate-glutathione cycle may then compensate for the limited capacity of the xanthophyll cycle, inducing an increase in the size of ascorbate and glutathione pool, as experimentally demonstrated in the brown alga *Sargassum thunbergii* (Nan et al., 2016). The simultaneous analysis of biochemical and photosynthetic parameters measured in thalli at the top of and beneath the canopy at the end of emersion (Figure 6) suggests that coordination between the xanthophyll and the ascorbate-glutathione cycles varies across seasons rather than during low tide. In general, no changes in ascorbate and glutathione content were observed during the emersion period; the occasional changes occurred in thalli both at the top of and beneath the canopy, suggesting a response to environmental conditions prevailing before emersion. Accumulation of hydrogen peroxide (H_2O_2) was nevertheless observed on one occasion at the top of the canopy, indicating that the ascorbate and glutathione pools were insufficient to scavenge H_2O_2 during this particular emersion period on 13 August 2018 (Exp F).

Conclusion

Measuring the photosynthetic performance of isolated thallus pieces, Jueterbock *et al.* (2014) suggested that the cold-temperate *F. serratus* physiology lacks the plasticity to respond to the thermal extremes predicted in the near future. The present study shows the importance of the dampening canopy

effect as well as biochemical acclimation for the physiology of this species and its ability to withstand environmental stresses. *F. serratus* canopies alter the environmental conditions and mitigate the levels of stress experienced in the lower layers of the same stand during emersion, whereas various acclimation strategies allow the adjustment of its photosynthetic capacity. Oxidative stress was nevertheless recorded once, presumably in response to recurrent heat stress. The potential of this foundation species to respond to frequent heat waves — predicted to occur in the future as a result of climate change — remains to be determined. If unable to adapt, the species could disappear, that would have catastrophic consequences on the whole community leading to the impoverishment of the coastal system.

Data accessibility

Data are available online: http://doi.org/10.5281/zenodo.5113898

Supplementary material

Script and codes are available online: http://doi.org/10.5281/zenodo.5113898

Acknowledgements

Conflict of interest disclosure

The authors declare that they have no financial conflict of interest with the content of this article.

References

Alvarez-Losada, O., Arrontes, J., Martinez, B., Fernandez, C., & Viejo, R. M. (2020). A regime shift in intertidal assemblages triggered by loss of algal canopies: a multidecadal survey. *Marine Environmental Research, 160*, 104981. https://doi.org/10.1016/j.marenvres.2020.104981

Arsalane, W., Rousseau, B., & Duval, J. C. (1994). Influence of the pool size of the xantophyll cycle on the effect of light stress in a Diatom: competition between photoprotection and photoinhibition. *Photochemistry and Photobiology, 60*(3), 237-243. https://doi.org/10.1111/j.1751-1097.1994.tb05097.x

Bilger, W., & Bjorkman, O. (1990). Role of the xanthophyll cycle in photoprotection elucidated by measurement in the light-induced absorbance changes, fluorescence and photosynthesis in leaves of *Hedera canariensis*. *Photosynthesis Research, 25*(3), 173-185. https://doi.org/10.1007/bf00033159

Binzer, T., & Sand-Jensen, K. (2002). Production in aquatic macrophyte communities: A theoretical and empirical study of the influence of spatial light distribution. *Limnology and Oceanography, 47*(6), 1742-1750. https://doi.org/10.4319/lo.2002.47.6.1742

Bordeyne, F., Migné, A., & Davoult, D. (2015). Metabolic activity of intertidal *Fucus spp*. communities: evidence for high aerial carbon fluxes displaying seasonal variability. *Marine Biology, 162*(10), 2119-2129. https://doi.org/10.1007/s00227-015-2741-6

Bordeyne, F., Migné, A., & Davoult, D. (2017). Variation of fucoid community metabolism during the tidal cycle: Insights from *in situ* measurements of seasonal carbon fluxes during emersion and immersion. *Limnology and Oceanography, 62*(6), 2418-2430. https://doi.org/10.1002/lno.10574

Bordeyne, F., Migné, A., Plus, M., & Davoult, D. (2020). Modelling the annual primary production of an intertidal brown algal community based on *in situ* measurements. *Marine Ecology Progress Series, in press*.

Bulleri, F. (2009). Facilitation research in marine systems: state of the art, emerging patterns and insights for future developments. *Journal of Ecology, 97*(6), 1121-1130. https://doi.org/10.1111/j.1365-2745.2009.01567.x

Casado-Amezua, P., Araujo, R., Barbara, I., Bermejo, R., Borja, A., Diez, I., . . . Martinez, B. (2019). Distributional shifts of canopy-forming seaweeds from the Atlantic coast of Southern Europe. *Biodiversity and Conservation, 28*(5), 1151-1172. https://doi.org/10.1007/s10531-019-01716-9

Chapman, A. R. O. (1995). Functional ecology of fucoid algae: 23 years of progress. *Phycologia, 34*(1), 1-32. https://doi.org/10.2216/i0031-8884-34-1-1.1

Connan, S., Deslandes, E., & Gall, E. A. (2007). Influence of day-night and tidal cycles on phenol content and antioxidant capacity in three temperate intertidal brown seaweeds. *Journal of Experimental Marine Biology and Ecology, 349*(2), 359-369. https://doi.org/10.1016/j.jembe.2007.05.028

Connan, S., Goulard, F., Stiger, V., Deslandes, E., & Gall, E. A. (2004). Interspecific and temporal variation in phlorotannin levels in an assemblage of brown algae. *Botanica Marina, 47*(5), 410-416. https://doi.org/10.1515/bot.2004.057

Contreras, L., Moenne, A., & Correa, J. A. (2005). Antioxidant responses in *Scytosiphon lomentaria* (Phaeophyceae) inhabiting copper-enriched coastal environments. *Journal of Phycology, 41*(6), 1184-1195. https://doi.org/10.1111/j.1529-8817.2005.00151.x

Crowe, T. P., Cusson, M., Bulleri, F., Davoult, D., Arenas, F., Aspden, R., . . . Jenkins, S. R. (2013). Large-scale variation in combined impacts of canopy loss and disturbance on community structure and ecosystem functioning. *Plos One, 8*(6), e66238. https://doi.org/10.1371/journal.pone.0066238

Davison, I. R., & Pearson, G. A. (1996). Stress tolerance in intertidal seaweeds. *Journal of Phycology, 32*(2), 197-211. https://doi.org/10.1111/j.0022-3646.1996.00197.x

Fernandez-Marin, B., Miguez, F., Maria Becerril, J., & Ignacio Garcia-Plazaola, J. (2011). Activation of violaxanthin cycle in darkness is a common response to different abiotic stresses: a case study in *Pelvetia canaliculata*. *Bmc Plant Biology, 11*. https://doi.org/10.1186/1471-2229-11-181

Fernandez, A., Arenas, F., Trilla, A., Rodriguez, S., Rueda, L., & Martinez, B. (2015). Additive effects of emersion stressors on the ecophysiological performance of two intertidal seaweeds. *Marine Ecology Progress Series, 536*, 135-147. https://doi.org/10.3354/meps11401

Flores-Molina, M. R., Thomas, D., Lovazzano, C., Nunez, A., Zapata, J., Kumar, M., . . . Contreras-Porcia, L. (2014). Desiccation stress in intertidal seaweeds: Effects on morphology, antioxidant responses and photosynthetic performance. *Aquatic Botany, 113*, 90-99. https://doi.org/10.1016/j.aquabot.2013.11.004

Genty, B., Briantais, J.-M., & Baker, N. R. (1989). The relationship between the quantum yield of photosynthetic electron transport and quenching of chlorophyll fluorescence. *Biochimica et Biophysica Acta, 990*, 87-92. https://doi.org/10.1016/S0304-4165(89)80016-9

Hanelt, D. (1996). Photoinhibition of photosynthesis in marine macroalgae. *Scientia Marina, 60*, 243-248.

Harker, M., Berkaloff, C., Lemoine, Y., Britton, G., Young, A. J., Duval, J. C., . . . Rousseau, B. (1999). Effects of high light and desiccation on the operation of the xanthophyll cycle in two marine brown algae. *European Journal of Phycology, 34*(1), 35-42. https://doi.org/10.1017/s0967026299001924

Hodges, D. M., Andrews, C. J., Johnson, D. A., & Hamilton, R. I. (1996). Antioxidant compound responses to chilling stress in differentially sensitive inbred maize lines. *Physiologia Plantarum, 98*, 685-692. https://doi.org/10.1111/j.1399-3054.1996.tb06672.x

Huppertz, K., Hanelt, D., & Nultsch, W. (1990). Photoinhibition of photosynthesis in the marine brown alga *Fucus serratus* as studied in field experiments. *Marine Ecology-Progress Series, 66*(1-2), 175-182. https://doi.org/10.3354/meps066175

Jueterbock, A., Kollias, S., Smolina, I., Fernandes, J. M. O., Coyer, J. A., Olsen, J. L., & Hoarau, G. (2014). Thermal stress resistance of the brown alga *Fucus serratus* along the North-Atlantic coast:

Acclimatization potential to climate change. *Marine Genomics, 13*, 27-36. https://doi.org/10.1016/j.margen.2013.12.008

Jueterbock, A., Tyerbghein, L., Verbruggen, H., Coyer, J. A., Olsen, J. L., & Hoarau, G. (2013). Climate change impact on seaweed meadow distribution in the North Atlantic rocky intertidal. *Ecology and Evolution, 3*(5), 1356-1373. https://doi.org/10.1002/ece3.541

Koch, K., Thiel, M., Hagen, W., Graeve, M., Gomez, I., Jofre, D., . . . Bischof, K. (2016). Short- and long-term acclimation patterns of the giant kelp *Macrocystis pyrifera* (Laminariales, Phaeophyceae) along a depth gradient. *Journal of Phycology, 52*(2), 260-273. https://doi.org/10.1111/jpy.12394

Lee, M. Y., & Shin, H. W. (2003). Cadmium-induced changes in antioxidant enzymes from the marine alga *Nannochloropsis oculata*. *Journal of Applied Phycology, 15*, 13-19. https://doi.org/10.1023/A:1022903602365

Lichtenberg, M., & Kuhl, M. (2015). Pronounced gradients of light, photosynthesis and O_2 consumption in the tissue of the brown alga *Fucus serratus*. *New Phytologist, 207*(3), 559-569. https://doi.org/10.1111/nph.13396

Mancuso, F. P., Messina, C. M., Santulli, A., Laudicella, V. A., Giommi, C., Sara, G., & Airoldi, L. (2019). Influence of ambient temperature on the photosynthetic activity and phenolic content of the intertidal *Cystoseira compressa* along the Italian coastline. *Journal of Applied Phycology, 31*(5), 3069-3076. https://doi.org/10.1007/s10811-019-01802-z

Mann, K. H. (1973). Seaweeds: their productivity and strategy for growth. *Science, 182*(4116), 975-981. https://doi.org/10.1126/science.182.4116.975

Mannino, A. M., Vaglica, V., Cammarata, M., & Oddo, E. (2016). Effects of temperature on total phenolic compounds in *Cystoseira amentacea* (C. Agardh) Bory (Fucales, Phaeophyceae) from southern Mediterranean Sea. *Plant Biosystems, 150*(1), 152-160. https://doi.org/10.1080/11263504.2014.941033

Martinez, B., Arenas, F., Rubal, M., Burgues, S., Esteban, R., Garcia-Plazaola, I., ... Viejo, R. M. (2012). Physical factors driving intertidal macroalgae distribution: physiological stress of a dominant fucoid at its southern limit. *Oecologia, 170*(2), 341-353. https://doi.org/10.1007/s00442-012-2324-x

Maxwell, K., & Johnson, G. N. (2000). Chlorophyll fluorescence - a practical guide. *Journal of Experimental Botany, 51*(345), 659-668. https://doi.org/10.1093/jexbot/51.345.659

Migné, A., Davoult, D., Spilmont, N., Menu, D., Boucher, G., Gattuso, J.-P., & Rybarczyk, H. (2002). A closed-chamber CO_2-flux method for estimating intertidal primary production and respiration under emersed conditions. *Marine Biology, 140*(4), 865-869. https://doi.org/10.1007/s00227-001-0741-1

Migné, A., Golléty, C., & Davoult, D. (2015). Effect of canopy removal on a rocky shore community metabolism and structure. *Marine Biology, 162*(2), 449-457. https://doi.org/10.1007/s00227-014-2592-6

Monteiro, C., Zardi, G. I., McQuaid, C. D., Serrao, E. A., Pearson, G. A., & Nicastro, K. R. (2017). Canopy microclimate modification in central and marginal populations of a marine macroalga. *Marine Biodiversity, 49*(1), 415-424. https://doi.org/10.1007/s12526-017-0824-y

Nan, G. N., Zhang, Q. S., Sheng, Z. T., & Zhang, D. (2016). Coordination between xanthophyll cycle and antioxidant system in *Sargassum thunbergii* (Sargassaceae, Phaeophyta) in response to high light and dehydration stresses. *Journal of Applied Phycology, 28*(4), 2587-2596. https://doi.org/10.1007/s10811-016-0791-x

Niell, F. X. (1977). Rocky intertidal benthic systems in temperate seas: a synthesis of their functional performances. *Helgolander Wissenschaftliche Meeresuntersuchungen, 30*(1-4), 315-333. https://doi.org/10.1007/bf02207844

Nielsen, H. D., & Nielsen, S. L. (2010). Adaptation to high light irradiances enhances the photosynthetic Cu^{2+} resistance in Cu^{2+} tolerant and non-tolerant populations of the brown macroalgae *Fucus serratus*. *Marine Pollution Bulletin, 60*(5), 710-717. https://doi.org/10.1016/j.marpolbul.2009.11.025

Pearson, G. A., Lago-Leston, A., & Mota, C. (2009). Frayed at the edges: selective pressure and adaptive response to abiotic stressors are mismatched in low diversity edge populations. *Journal of Ecology, 97*(3), 450-462. https://doi.org/10.1111/j.1365-2745.2009.01481.x

Ragan, M. A., & Jensen, A. (1978). Quantitative studies on brown alagal phenols .2. Seasonal variation in polyphenol content of *Ascophyllum nodosum* (L.) Le Jol. and *Fucus vesiculosus* (L.). *Journal of*

Experimental Marine Biology and Ecology, 34(3), 245-258. https://doi.org/10.1016/s0022-0981(78)80006-9

Ratkevicius, N., Correa, J. A., & Moenne, A. (2003). Copper accumulation, synthesis of ascorbate and activation of ascorbate peroxidase in *Enteromorpha compressa* (L.) Grev. (Chlorophyta) from heavy metal-enriched environments in northern Chile. *Plant Cell and Environment, 26*(10), 1599-1608. https://doi.org/10.1046/j.1365-3040.2003.01073.x

Sand-Jensen, K., Binzer, T., & Middelboe, A. L. (2007). Scaling of photosynthetic production of aquatic macrophytes – a review. *Oikos, 116*(2), 280-294. https://doi.org/10.1111/j.0030-1299.2007.15093.x

Tait, L. W., Hawes, I., & Schiel, D. R. (2017). Integration of chlorophyll a fluorescence and photorespirometry techniques to understand production dynamics in macroalgal communities. *Journal of Phycology, 53*(3), 476-485. https://doi.org/10.1111/jpy.12524

Tait, L. W., & Schiel, D. R. (2011). Dynamics of productivity in naturally structured macroalgal assemblages: importance of canopy structure on light-use efficiency. *Marine Ecology Progress Series, 421*, 97-107. https://doi.org/10.3354/meps08909

Valdivia, N., Golléty, C., Migné, A., Davoult, D., & Molis, M. (2012). Stressed but stable: canopy loss decreased species synchrony and metabolic variability in an intertidal hard-bottom community. *Plos One, 7*(5), e36541. https://doi.org/10.1371/journal.pone.0036541

van Hees, D. H., Olsen, Y. S., Wernberg, T., Van Alstyne, K. L., & Kendrick, G. A. (2017). Phenolic concentrations of brown seaweeds and relationships to nearshore environmental gradients in Western Australia. *Marine Biology, 164*(4). https://doi.org/10.1007/s00227-017-3115-z

Yates, J. L., & Peckol, P. (1993). Effects of nutrient availability and herbivory on polyphenolics in the seaweed *Fucus vesiculosus*. *Ecology, 74*(6), 1757-1766. https://doi.org/10.2307/1939934

Appendix

Appendix 1. Initial (i) and final (f) values (mean ± se in µmol g_{DW}^{-1}, n = 3) of hydrogen peroxide (H_2O_2), ascorbate (Asc) and glutathione (Glu) measured in thalli from different layers of the canopy (top, bottom or intermediate) on seven dates

Date	layer	H_2O_{2i}	H_2O_{2f}	Asc_i	Asc_f	Glu_i	Glu_f
2017.05.26	top	3.14 ± 0.05	2.75 ± 0.45	10.24 ± 1.60	9.58 ± 1.07	0.87 ± 0.12	1.38 ± 0.13
	bottom	3.05 ± 0.53	2.66 ± 0.28	9.96 ± 2.75	10.33 ± 2.77	0.92 ± 0.02	1.35 ± 0.21
2017.05.27	top	3.66 ± 0.38	3.26 ± 0.10	11.22 ± 2.40	12.05 ± 1.82	1.48 ± 0.13	1.34 ± 0.05
	bottom	3.57 ± 0.33	3.93 ± 0.19	5.49 ± 0.77	8.26 ± 1.18	1.35 ± 0.37	1.35 ± 0.06
2017.08.22	top	3.54 ± 0.22	3.48 ± 0.32	6.49 ± 0.29	9.17 ± 1.69	0.75 ± 0.04	0.71 ± 0.09
	bottom	3.53 ± 0.68	4.86 ± 0.46	4.12 ± 0.17	9.27 ± 0.69	0.64 ± 0.12	0.91 ± 0.13
2017.08.23	top	3.55 ± 0.77	4.12 ± 0.38	5.77 ± 0.86	7.31 ± 1.45	0.28 ± 0.02	0.36 ± 0.10
	bottom	3.47 ± 0.44	3.24 ± 0.61	6.95 ± 1.57	6.09 ± 3.51	0.23 ± 0.09	0.36 ± 0.18
2017.12.04	top	3.13 ± 0.31	3.31 ± 0.32	10.86 ± 1.27	8.40 ± 0.73	0.96 ± 0.12	0.93 ± 0.04
	bottom	3.25 ± 0.29	3.41 ± 0.10	8.84 ± 1.11	4.13 ± 2.06	0.86 ± 0.09	0.79 ± 0.20
2017.12.05	top	3.01 ± 0.44	2.77 ± 0.17	10.74 ± 1.06	8.02 ± 1.04	0.76 ± 0.07	0.66 ± 0.16
	int.	4.32 ± 0.35	4.37 ± 0.73	6.40 ± 2.64	5.00 ± 1.58	0.52 ± 0.20	0.46 ± 0.08
2018.08.13	top	3.85 ± 0.41	5.02 ± 0.64	11.40 ± 1.13	10.26 ± 2.43	0.85 ± 0.04	0.96 ± 0.03
	int.	2.60 ± 0.38	2.99 ± 0.26	8.45 ± 0.33	9.09 ± 1.35	0.96 ± 0.15	1.14 ± 0.09
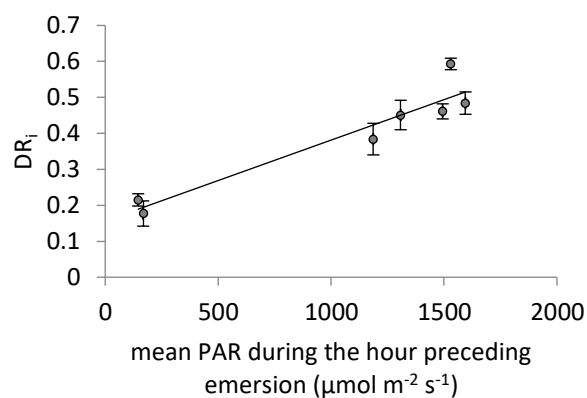
Appendix 2. Relationship between de-epoxidation ratio at the beginning of emersion (DRi, mean ± se, n = 6) and the incident light during the hour preceding emersion (as mean photosynthetically available radiation, PAR, n = 60)